

# Topological dynamics of optical singularities in speckle-fields induced by photorefractive scattering in a $\text{LiNbO}_3:\text{Fe}$ crystal\*

V.I. Vasil'ev, M.S. Soskin

**Abstract.** A natural singular dynamics of elliptically polarised speckle-fields induced by the ‘optical damage’ effect in a photorefractive crystal of lithium niobate by a passing beam of a helium–neon laser is studied by the developed methods of singular optics. For the polarisation singularities (C points), a new class of chain reactions, namely, singular chain reactions are discovered and studied. It is shown that they obey the topological charge and sum Poincare index conservation laws. In addition, they exist for all the time of crystal irradiation. They consist of a series of interlocking chains, where singularity pairs arising in a chain annihilate with singularities from neighbouring independently created chains. Less often singular ‘loop’ reactions are observed where arising pairs of singularities annihilate after reversible transformations in within the boundaries of a single speckle. The type of a singular reaction is determined by a topology and dynamics of the speckles, in which the reactions are developing.

**Keywords:** optical polarisation singularities, C points, optical diabols, Stokes-polarimetry, topological reactions.

## 1. Introduction

Singular optics is a new quickly developing branch of optics, which studies optical singularities – the structures with discrete amplitude and polarisation states of coherent light fields [1–3]. Genesis and evolution of the singularities is a subject of investigations of dynamic singular optics [4]. Methods developed on this basis made possible real-time studying the genesis of optical singularities and evolution mechanisms in developing speckle-fields [5–7]. As is known, optical speckle-fields with random variations in amplitude, phase, and polarisation are realised, for example, in laser radiation passing through scattering media or turbulent atmosphere. If at a certain point of a speckle-field the phase fluctuations reach  $2\pi$  then the field amplitude vanishes in the result of destructive interference. Such points become centres of optical vortices with a helical wave front [2].

In elliptically polarised fields, to a vortex with the left-hand (right-hand) polarisation correspond singular C points

with the right-hand (left-hand) circular polarisation. These points form around themselves the three types of morphological organisation of nearest polarisation ellipses: star (S), monstar (M), lemon (L) with three for S, M, and one for L line segments, along which the major axes of ellipses are oriented [2]. In this case, the surface of length distribution for major ( $a$ ) and minor ( $b$ ) axes of polarisation ellipses (optical diabols) looks like right (elliptic, E) or oblique (hyperbolic, H) cones directed up and down with a common vertex at C points and the Poincare indices of +1 and 0, respectively [8–10]. With the allowance made for the three morphology types of C point there are six combinations with the diabol topology: E(S), E(M), E(L), H(S), H(M), H(L) [10], which will be employed in describing experimental results. It is reasonable to describe the structure of speckles by the distribution of the minor axes length  $b(x, y)$ . Their shape is represented by smooth contour lines except for the h-line contours, which cross the diabol vertices (C points) and exhibit a kink due to the conical shape of the cross section around the diabol vertex [10].

Singular dynamics of developing speckle-fields is of principal scientific and practical interest; it is entirely determined by an evolution of the structure of the speckles involved. Presently the best effect suitable for studying generic processes of topologic and morphologic transformations of light-field singularities is the evolution of a speckle-field of scattered radiation induced in photorefractive crystals by a passing laser beam (nonlinear effect of optical damage [11]). Earlier, it was theoretically shown that nonstationary scalar dislocations of a wave front arise in pulsed sound fields with a complex wave front that are generated by a pulsed piston emitter [12]. They can move in direct and backward directions and annihilate in pairs. The calculated reactions were quasi-one-dimensional unlike to three-dimensional reactions in dynamic optical speckle-fields [8].

The present work is mainly aimed at establishing a scenario and spatial-temporal laws of burning, evolution and annihilation of the C points in the course of evolution of dynamic speckle-fields generating them.

## 2. Classification of topological reactions

The experimental setup and measuring methods are thoroughly described in [8]. A two-stage recording of orthogonally polarised induced noise lattices realised a speckle-field with random elliptical polarisation. Each Stokes component was recorded for 20 ms. All necessary rotations of analysing optical elements were performed with a closed laser beam for eliminating field evolution during the readjustment. The intensity distribution of speckle-fields was detected by a

\* Reported at the ‘Laser Optics’ conference (St. Petersburg, Russia, June 2012).

V.I. Vasil'ev, M.S. Soskin. Institute of Physics, National Academy of Sciences of Ukraine, prosp. Nauki 46, 03028 Kiev, Ukraine; e-mail: vv@iop.kiev.ua, marat.soskin@gmail.com

Received 24 October 2012; revision received 12 November 2012  
Kvantovaya Elektronika 43 (2) 125–129 (2013)  
Translated by N.A. Raspopov

CCD-camera and processed according to the adopted noise filtering algorithms thoroughly described in [13]. The total duration of crystal irradiation and, consequently, of speckle-field development was  $\sim 60$  min, to the end of the irradiation the optical breakdown processes actually saturated. The prescribed time interval between successive frames  $t = 15$  s provided a detailed tracing of the evolution of the topologic and morphologic structure in a chosen fraction of the speckle-field by means of Stokes polarimetry [14].

A typical example of a speckle-structure of a developing elliptic speckle-field is shown in Fig. 1. In agreement with theory [10], all hyperbolics reside at a speckle slope and ellipses – on the speckle vertices.

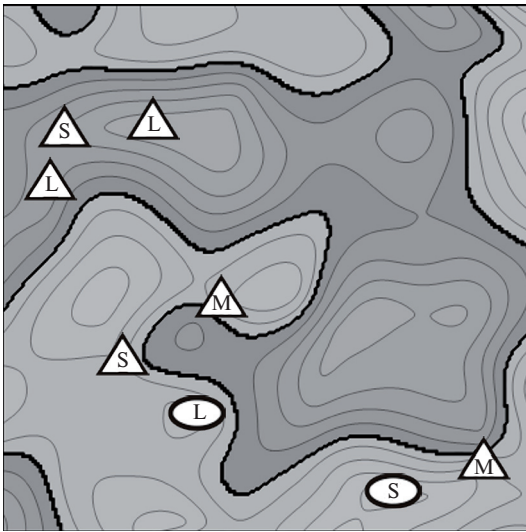


**Figure 1.** Distribution of ellipse minor axes  $b(x, y)$  of a speckle-field fragment. Light (dark) domains have right-hand (left-hand) polarisation and are separated by L-lines with a linear polarisation (bold lines) [2]. Thin grey lines describe the speckle shape. Markers show positions of C points. Elliptic (ellipse) and hyperbolic (triangle) markers correspond to two possible types of optical diabolos [10].

According to the topology of a singular elliptic speckle-field there are four possible combinations of neighbouring pairs of hyperbolics and ellipses. Their measured structures are presented in Fig. 2. One can see that all united surfaces  $a(x, y)$  and  $b(x, y)$  for neighbouring singularities are smooth even with opposite polarisations of the neighbouring C points (Fig. 2d). This result seems natural because the axes of ellipses are scalars independent of the field polarisation. According to general laws of topology and singular optics, all evolution processes of speckle-fields and the generated singularities should occur with preserving the sum Poincaré index  $I_p$  of the field and the topologic charge of singularities [11] ( $I_p = +1$  at a speckle vertex and  $I_p = 0$  at all points at the speckle slope).

This is directly confirmed by the observation of burning (annihilation) of only hyperbolic H(S)–H(M) pairs in a developing speckle-field, because this is the only scenario preserving the sum topologic charge of the system [2] and the sum Poincaré index  $I_p = 0$  at the pair burning site [10] with minimal arising field phase gradients.

We have discovered and studied singular topologic chain reactions. Those include a time-unlimited series of meshing segments, which are realised in developing speckle-fields (Fig. 3a). The reaction ‘fuel’ is an instantaneous pairwise

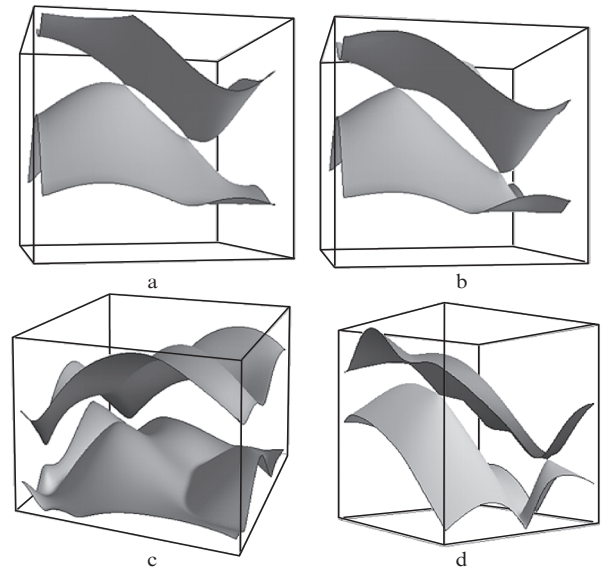


**Figure 2.** Distributions of major  $a$  (minor  $b$ ) axes of the polarisation ellipses on the top (bottom) surfaces: a pair of hyperbolics H(L)–H(S) on the slope of a speckle (a), transformation of the top (bottom) hyperbolic H(L) to elliptic E(L) (drift to the speckle base) in shifting the top C point to a speckle maximum (b), the surfaces  $a(x, y)$  and  $b(x, y)$  do not touch if there is no singularity (c), the H(L)–E(S) pair at a neighbouring field sites with opposite circular polarisation (d).

burning of scalar and polarisation optical singularities under the compliance of the sum topological field charge [2]. There are also coexisting less frequent isolated closed trajectories (‘loops’) (Fig. 3b), which minimally participate in the topological evolution of the speckle-field.

Chain reactions of elliptical speckle-fields exhibit a larger topological variety, which is related to existence of the above

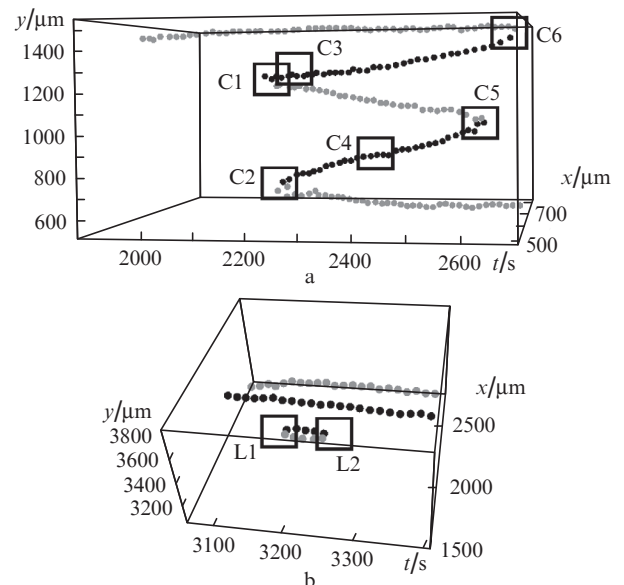


**Figure 3.** Parameters of chain (a) and loop (b) reactions. Time  $t$  is counted from the instant of irradiation of a lithium niobate crystal;  $x, y$  are the coordinates of a singularity on the input screen of a CCD-camera.

mentioned six possible combinations of morphological forms of C points and the accompanying optical diabolos. However, their general spatial structure is strictly fixed. The successive segments are interlocked by trajectories of H(S)-singularities, the input and output trajectories being alternately the upper and lower with respect to arising chains (Fig. 3a). There are also coexisting trajectories of H(M)-points, which in the process of evolution leave H(S)-points and transfer to a more stable form [H(L), E(M), or E(L)]. A simpler loop reaction is realised within a separate speckle with a single maximum in the distribution of the short axis of polarization ellipses  $b(x, y)$  (Fig. 3b).

### 3. Loop reactions

In a simplest case, a loop reaction lasts for at most 100 s and takes only four frames from the instant of C point pair burning at  $t = 1365$  s until their annihilation at  $t > 1425$  s (Fig. 4). In Fig. 4, one can see an arrangement of hyperbolics H(S)–H(M) on the corresponding speckle along with their morphological lines at the instants of burning, evolution, and annihilation. In agreement with the principle of minimisation of necessary speckle shape variations in origin and evolution of a singular reaction, the burning of a C point pair always occurs on the slope of an initial smooth speckle without singularities (Fig. 4a) in the form of a hyperbolic H(S)–H(M) pair with the actually parallel side morphological lines (Fig. 4b). In this case, two morphological lines of H(M) are closer to each other due to an asymmetry of real speckles. Since the M-form is unstable, it rapidly transfers to a stable hyperbolic H(L) (Fig. 4c), which moves to the speckle maximum. Then it walks down along the speckle slope (Fig. 4d). In getting close to the actually stationary hyperbolic H(S), the hyperbolic H(L) transfers to a hyperbolic H(M) with three morphological lines, similarly to the case of a C point pair

burning (Fig. 4e). In this case, the mean morphological line is likewise asymmetric as it was at the beginning of a loop reaction evolution; the external side lines are actually parallel to the corresponding lines of the H(S) hyperbolic. Then the H(S)–H(M) pair annihilates (Fig. 4f). A comparison of the first (Fig. 4a) and last (Fig. 4f) frames of the series reveals that the shape of the initial speckle without singularities remains almost unchanged in the course of the loop reaction. Note that in the process of the loop reaction, the singularity H(S) remains almost immovable. Obviously, closed chain reactions, which develop within a separate speckle, do not participate in general evolution dynamics of speckle-fields and may be classified as ‘topological impurities’.

### 4. Chain reactions

Separate segments of chain reactions exhibit quite different sequences of topological transformations. It was found that they strictly obey the following laws: a free motion of hyperbolics H(L) over the speckle-field, a transfer of the hyperbolic H(S) from the speckle wherein it was burn to a neighbouring speckle containing H(L), with which the former may annihilate. The remaining and arising C points continue development of the time-unlimited chain reaction.

Below (Figs 5 and 6), two typical examples of such development are presented. Similarly to Fig. 4, minimal necessary data about the speckle-field are given: the speckle contours, topology and morphology of C point, and contours of the h-lines crossing them.

Main stages of the evolution of a separate segment of a chain reaction are shown in Fig. 5. Time is counted from the start of the chain measurements. At  $t = 15$  s (Fig. 5a), the initial structure of the fragment under investigation is presented for a developing speckle-field, which comprises a complicated speckle with three local maxima and the correspond-

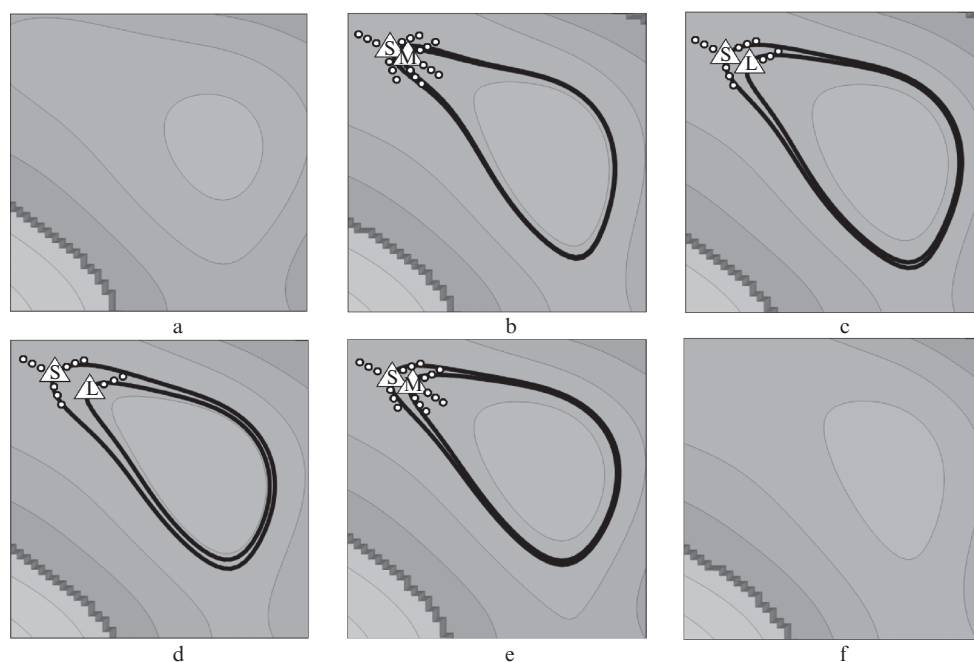


**Figure 4.** Loop chain reaction in the limits of a single speckle: the initial speckle ( $t = 1350$  s) (a), creation of a H(S)–H(M) pair ( $t = 1365$  s) (b), transfer of H(M) to H(L) with distance from H(S) ( $t = 1380$  s) (c), ascent of H(L) to a vertex of the speckle ( $t = 1395$  s) (d), descent of H(L) with a return to H(M) ( $t = 1425$  s) (e), annihilation of H(S)–H(M) ( $t = 1455$  s) (f).

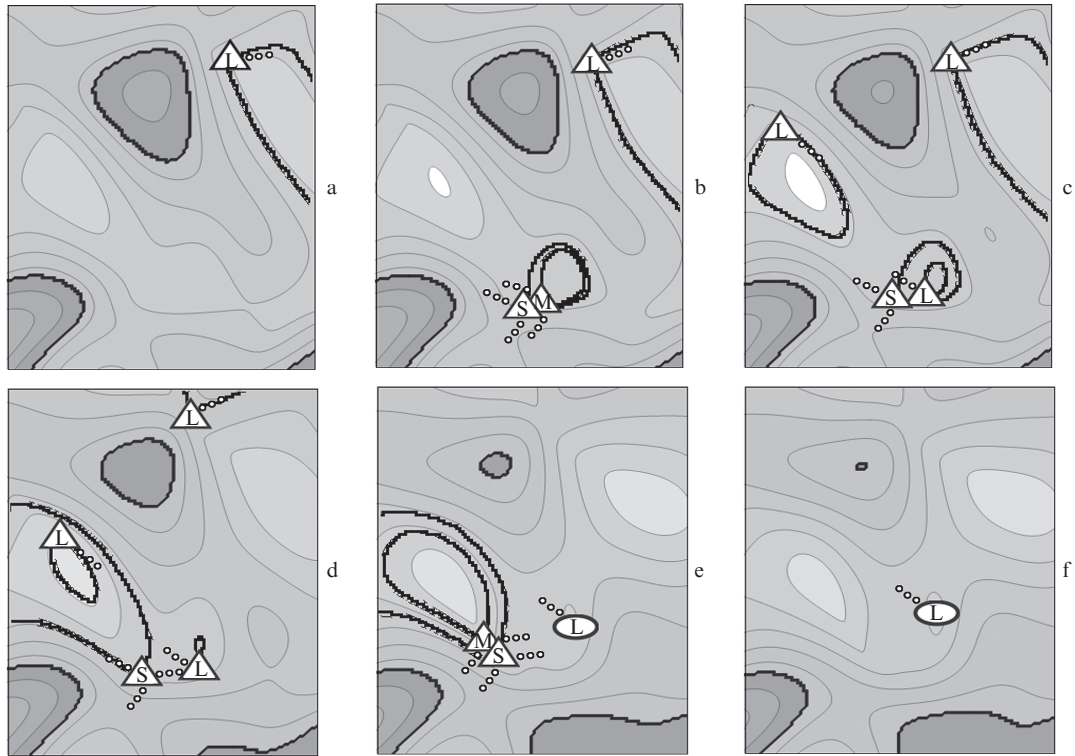


**Figure 5.** Separate segment of a chain reaction with various shapes of C points (example 1). The field structure is described by contour lines (bold h-lines cross the C points).

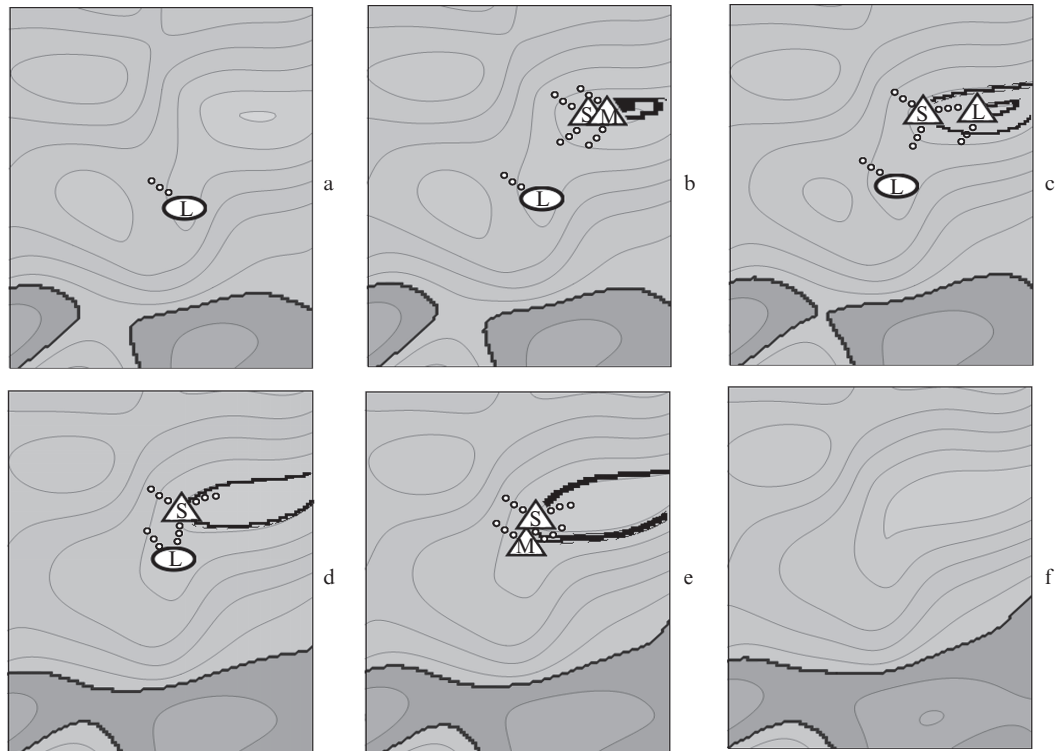


**Figure 6.** Separate segment of a chain reaction with various shapes of C points (example 2).

ing local speckles. In the upper local speckle, there exist the only hyperbolic H(L), which has passed from a neighbouring segment of the chain reaction in full agreement with the the-

ory [10], which predicts that a hyperbolic H(L) with  $I_p = 0$  freely moves in a developing speckle-field. At  $t = 30$  s (Fig. 5b), in the bottom local speckle a standard hyperbolic H(S)–H(M)

pair arises in the same domain as in the case of the loop reaction (Fig. 4b). A next step of the evolution at  $t = 45$  s (Fig. 5c) is also standard with a transformation of H(M) into H(L). At the same instant, a singularity H(L) arrives to a slope of the upper local speckle. The following evolution of the H(S)–H(L) pair is radically distinct from the loop reaction evolution. At  $t = 90$  s (Fig. 5d), the hyperbolic H(S) moves to the neighbouring upper speckle, where the hyperbolic H(L) simultaneously walks down in the opposite direction. At  $t = 165$  s (Fig. 5e), the rest hyperbolic L climbs over the vertex of the bottom local speckle transforming into the elliptic E(L). The hyperbolic H(L) in the left upper speckle closely approaches H(S) transforming as it should into H(M). Simultaneously, the upper single H(L) walks beyond the limits of the measured speckle-field fragment to other segments of the chain reaction. Finally at  $t = 180$  s (Fig. 5f), the hyperbolic H(S)–H(M) pair annihilates, and the single hyperbolic H(L) remains waiting for new singular pairs from next segments of the chain reaction. One can see that both the mechanisms are involved into the scenario of evolution of a separate segment of the chain reaction.

Another segment of the chain reaction starts at  $t = 285$  s (Fig. 6a) in the same fragment of the developing speckle-field, where a large speckle with three local maxima (speckles) resides. At the vertex of the small central local speckle one can see the elliptic E(L) remained from the previous segment. At  $t = 300$  s (Fig. 6b), a standard hyperbolic H(S)–H(M) pair is burnt at the slope of the upper local speckle. At  $t = 330$  s (Fig. 6c), the lower hyperbolic H(M) walks up the slope of the upper right speckle transforming into a hyperbolic H(L). In the process, the bottom speckle moves up with the elliptic E(L) at its vertex. At  $t = 375$  s (Fig. 6d), the left local speckle vanishes, the elliptic E(L) and hyperbolic H(S) become closer. Simultaneously the upper hyperbolic H(L) walks beyond the right limit of the fragment towards other segments of the chain reaction. The key topological transformation occurs at  $t = 390$  s (Fig. 6e) when the bottom speckle vanishes and the elliptic E(L) transforms into a hyperbolic H(M). As a result, the hyperbolics H(L) and H(S) reside very closely within the common speckle. Finally, they freely annihilate at  $t = 405$  s (Fig. 6f) and the considered fragment of the developing speckle-field temporarily loses singularities. One can see that in the latter case only free movement of hyperbolics over the speckle-field occurs.

## 5. Conclusions

The measured complete sets of singular point characteristics [4] made it possible to determine the corresponding realisation probabilities (Table 1). One can see that within the limits of measurement errors they coincide with the measurement data for the stationary speckle-field arising in laser beam scattering on tarnished glass and with the theoretically calculated static singular Gaussian fields [15]. This definitely indicates the ergodicity of a natural system of developing speckle-fields. As is known [16], the expectancy in ergodic systems is equal to the average value of a random variable. This is just the situation realised in dynamic and static elliptical speckle-fields.

Concluding we should stress that the topological reactions discussed differ from known nuclear and chemical chain reactions [17, 18]. The latter do not require conservation of the total number of particles involved. One more substantial difference is a production of ‘fuel’ for maintaining the topological chain reaction just in the process of its development in the result of burning new C point pairs.

**Table 1.** Statistics of morphological characteristics of dynamic and static polarisation optical singularities in elliptical speckle-fields.

Morphological type of singularity	Reaction probability		
	Dynamic speckle-fields (experiment) [4]	Static speckle-fields (experiment) [15]	Static speckle-fields (theory) [15]
E(S)	$0.23 \pm 0.015$	$0.253 \pm 0.005$	0.25
H(S)	$0.27 \pm 0.015$	$0.256 \pm 0.005$	0.25
E(L)	$0.24 \pm 0.015$	$0.2215 \pm 0.005$	0.2347
H(L)	$0.20 \pm 0.015$	$0.221 \pm 0.005$	0.2125
E(M)	$0.018 \pm 0.015$	$0.02 \pm 0.005$	0.0152
H(M)	$0.039 \pm 0.015$	$0.03 \pm 0.005$	0.0376

Obviously, the loop and chain reactions described may occur in developing singular wave fields of arbitrary nature with an arbitrary wavelength.

## References

1. Nye J.F., Berry M.V. *Proc. R. Soc. London. Ser. A*, **336**, 165 (1974).
2. Nye J.F. *Natural Focusing and Fine Structure of Light* (Bristol: Institute of Physics, 1999).
3. Soskin M.S., Vasnetsov M.V., in *Progress in Optics* (Amsterdam: Elsevier, 2001) Vol. 42, Ch. 4, p. 219.
4. Vasil'ev V., Soskin M. *Opt. Commun.*, **281**, 5527 (2008).
5. Vasil'ev V.I. *Proc. SPIE Int. Soc. Opt. Eng.*, **7613**, 7613OK (2010).
6. Vasil'ev V.I., Soskin M.S. *Proc. SPIE Int. Soc. Opt. Eng.*, **8274**, 8274OW (2012).
7. Vasil'ev V.I., Denisenko V.G., Egorov R.I., Slyusar V.V., Soskin M.S. *Kvantovaya Electron.*, **38**, 239 (2008) [*Quantum Electron.*, **38**, 239 (2008)].
8. Egorov R.I., Soskin M.S., Freund I. *Opt. Lett.*, **31**, 2048 (2006).
9. Freund I., Soskin M.S., Egorov R.I., Denisenko V. *Opt. Lett.*, **31**, 2381 (2006).
10. Freund I. *Opt. Commun.*, **272**, 293 (2007).
11. Odoulov S.G., Sturman B.I., in *Progress in Photorefractive Nonlinear Optics* (London – New York: Taylor & Francis, 2002).
12. Wright F.J., Berry M.V. *J. Acoust. Soc. Am.*, **75**, 733 (1984).
13. Vasil'ev V.I., Soskin M.S. *Ukr. J. Phys.*, **52**, 1123 (2007).
14. Born M., Volf E. *Principles of Optics* (Oxford: Pergamon, 1964; Moscow: Mir, 1970).
15. Flossmann F., O'Holleran K., Dennis M.R., Padgett M.J. *Phys. Rev. Lett.*, **100**, 203902 (2008).
16. Walters P. *An Introduction Ergodic Theory* (Berlin: Springer, 1982).
17. Semenov N.N. *Problemy khimicheskoi kinetiki* (Problems of Chemical Kinetics) (Moscow: Nauka, 1979).
18. Klimov A.N. *Yadernaya fizika i yadernye reaktory* (Nuclear Physics and Nuclear Reactors) (Moscow: Energoatomizdat, 1985).